PROCEEDINGS, Thirty-Ninth Workshop on Geothermal Reservoir Engineering
Stanford University, Stanford, California, February 24-26, 2014
SGP-TR-202

Comparing Induced Seismicity On Different Scales

C.E. Bachmann, W. Foxall and T. Daley

Lawrence Berkeley National Lab, Berkeley CA, USA

cebachmann@lbl.gov

Keywords: Induced seismicity, Paradox Valley, Brine Injection, Long-term Injection

ABSTRACT

The Paradox Valley Unit (PVU) is operated by the U.S. Bureau of Reclamation (USBR) and is built to control the water quality of the Dolores River - a feeder of the Colorado River. Brine is extracted along the river from several shallow wells. Before it is injected into a 4.8km deep well for long-term storage, it is filtered at a surface-treatment facility. The target zone of the injection is a subhorizontal formation of a Mississippian-age limestone. The first injection test started in 1991. Continuous injection started in 1996 and is still ongoing.

Micro-seismicity induced by the injection is monitored with the 15-station Paradox Valley Seismic Network operated by USBR, and more then 5700 events have been located during the 20 years since the start of injection. The locations of the seismic events provide crucial insights to the migration pathways of the injected fluid. In this study we analyze the seismicity up to the end of 2011, which does not include the magnitude 3.9 event that caused a temporary shut down of the PVU in January 2013. The largest event included in our study period is an event with M4.3 that occurred in May 2000. The majority (75%) of the events have magnitudes of 1 or smaller; only 74 events have magnitudes larger or equal to 2.5, of which only 4 are larger or equal to 3.5. About 80% of the seismicity occurred within 4km of the injection well. However, one zone more then 10 km away from the well first became active in late 2010, and more than 500 microearthquakes occurred within several weeks.

The goal of this study is to understand the processes occurring during a long-term subsurface fluid injection when there is no circulation. While other wastewater injection projects exist, none has been monitored as well as the Paradox Valley seismicity or has been going on for such a long time. The first step is to characterize in detail the frequency magnitude distributions (FMD) of the ongoing seismicity at Paradox Valley. We then infer the locations of several small faults from the seismicity and relate the b-values of the Gutenberg Richter relationship to those faults. We find an overall correlation between the orientation of the faults and the b-values. In addition, we investigate the influence of the different injection regimes on the behavior of the FMD and thus the b-value.

1. INTRODUCTION

It has been known for many years that human activity may induce earthquakes through processes related to mines, reservoirs, dams, geothermal projects and fluid and waste injection (e.g. Gupta, 2002; Simpson, 1986; Talwani, 1997). In recent years geothermal- and wastewater-related seismicity in particular has raised public concern (e.g. Ellsworth, 2013; Giardini, 2009; Keranen et al. 2013; Horton, 2012). Induced seismicity is also an issue for geological storage of CO_2 (GCS) because of the hypothesized potential for large events (Zoback and Goerlick, 2012). Commercial-scale GCS generally will involve much larger fluid volumes and time scales than geothermal or wastewater projects, but the few projects carried out to date have been on a smaller scale and have not induced significant seismicity. It is therefore necessary to either model the long-term behavior of GCS reservoirs or find proxies involving large injected volumes. One such project is the USBR's Paradox Valley Unit (PVU) in Colorado, which has been injecting brine into a deep well more or less continuously since 1996. The goal of the PVU is to extract brine from the shallow aquifer under the Paradox Valley (PV) and dispose of it by injection, thereby preventing it from flowing into the Colorado River and increasing its salinity. As large volumes of brine are injected into the subsurface for long-term storage, the PVU is a good candidate as a proxy to for GCS. The objective of injection of wastewater from unconventional oil and gas production activities is also long-term storage of large fluid volumes. However, most of those projects have not been carried out for long time periods, the seismicity has not been monitored by dedicated seismic networks, and site characterization has generally not been as extensive as for the PVU.

We carry out statistical analysis of the seismicity induced by the PV project, such as determining frequency-magnitude distributions. By comparing the results to those obtained from the Enhanced Geothermal Project in Basel, Switzerland in 2006, we explore the overall applicability of the statistical characterizations to different scales of time and injected volume and different geological settings. If the seismicity characteristics resulting from short- and long-term projects are similar, then the former, which are more numerous and for which more data are available, can be used to validate models seismicity and flow for GCS..

2. DATA

The PVU consists of several shallow wells (10- 100m deep) that extract brine along the Dolores River. Since the Dolores River is a tributary of the Colorado River, the brine contributes to downstream salinity, which would cause millions of dollars in damage if not remediated. The target horizon for brine disposal is a sub-horizontal Mississippian-age limestone formation at 4.3-4.8 km depth.

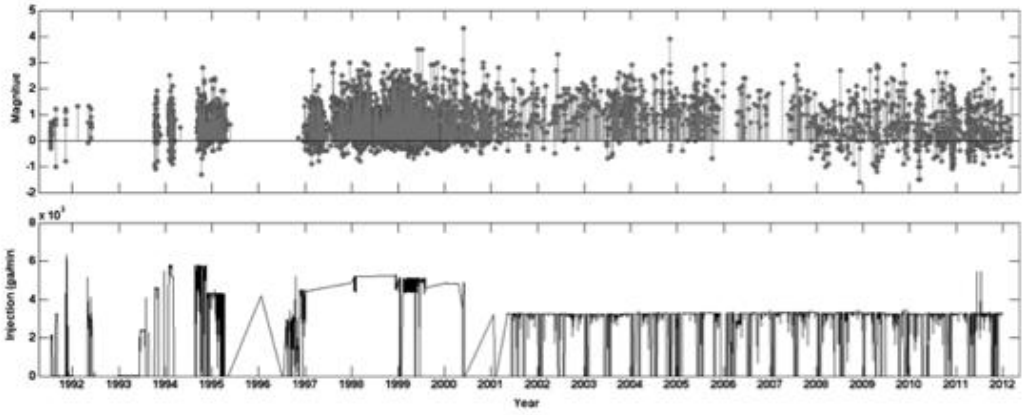

Figure 1: The evolution of seismicity (top panel), compared to the injection rate in gallons/minute (lower panel). While the injection tests lead to a direct seismic response, the seismicity is not correlated with the injection directly from 2001 on.

Figure 1 illustrates the changes in injections over time. The injection regime can be divided into two main periods, injection testing between July 1991 and April 1995 and continuous injection. The second period started in May 1996, and can be divided into four different phases (Ake et al. 2005):

- Phase I (22 July 1996–25 July 1999).
- Phase II (26 July 1999–23 June 2000).
- Phase III (24 June 2000–7 January 2002).
- Phase IV (8 January 2002–present).

Different average injection rates and pressures, and different ratios between injected brine and water characterize the different phases. Ake et al. only describe the phases up to the end of 2003, but as we see from Figure 1, there has been no substantial change in the average injection rate since then. Therefore, we extend Phase IV to the present, and include data until the end of 2012.

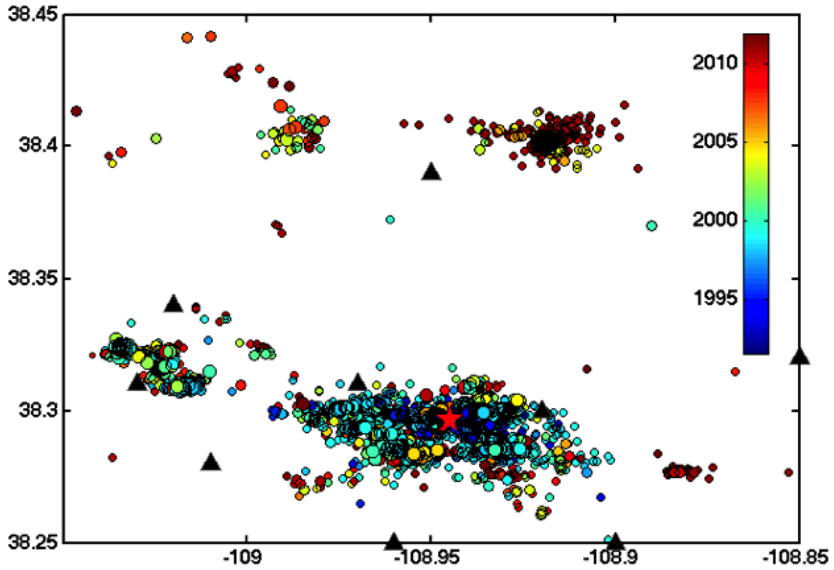

Figure 2: Location of the Paradox Valley seismicity. The seismic events are scaled by magnitude and color coded by year of occurrence. The injection well is shown by the red star and the subset of seismic stations closest to the well is shown by black triangles.

The seismicity was recorded by the Paradox Valley Seismic Network (PVSN), which consists of 23 stations active over different periods of time. The PVSN recorded close to 6,000 events since the beginning of the injection. Especially at the beginning, the seismic activity is closely related to the injection (Figure 1). The highest activity is seen once the continuous injection starts in 1996. After 2001 there is no longer a clear correlation between injection and seismicity rates and there is significantly less activity overall. This can be explained if we look at the injection phases defined above. In May 2000 the largest magnitude (M4.3) event at PV occurred. This event first caused a temporary 28-day shutdown of the project and then led to a reduced injection rate (Phase III) and later to a change in the brine-water ratio (Phase IV). The combination of those strategies led to a significant reduction in seismicity. This is also seen in the breakdown of the events per year (Figure 3, middle panel); most of the activity occurred from

1997 to 2000 and then it died down. There is an increase in activity in 2011, which corresponds to a newly active area north of the injection well (around 38.4N /108.91 W in Figure 2). Several hundred events occurred here within several days.

The events are mostly located close to the injection well, with 78% of the events occurring within 4km distance. Earthquake depths are also predominantly close to the targeted zone, but with some shallower and deeper outliers. There is no apparent activity between the seismicity clustered near the well and the 2011 cloud to the north, which suggests that the fluid migrated without accompanying sesimicty until it encountered a new set of faults. We concentrate our analysis on the main seismic cloud, but it is important to note that isolated zones of activity like the one to the north can occur during any project and it is difficult to predict and model this behavior.

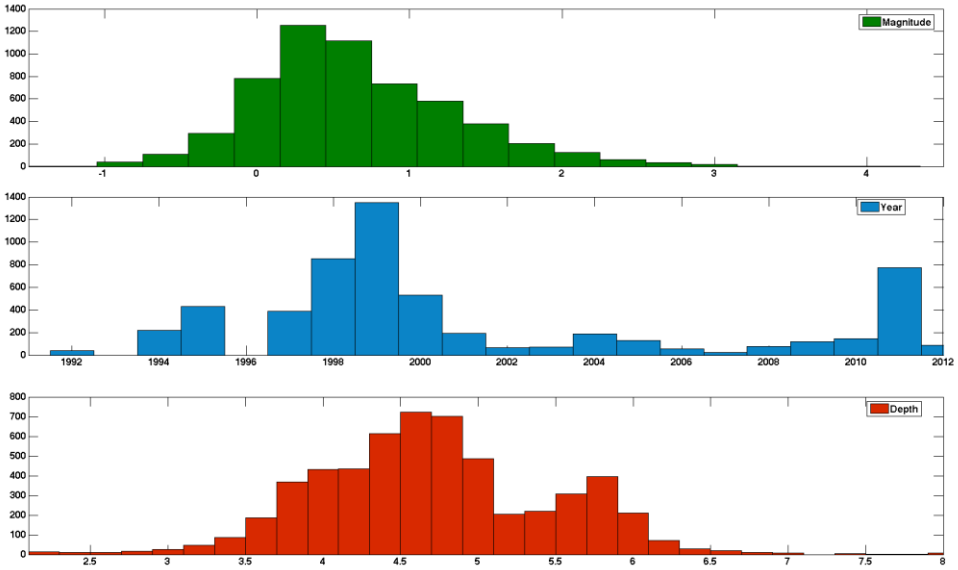

Figure 3: Statistical analysis of the distribution of magnitudes, years and depth of events.

The recorded seismic events are generally small, with magnitudes ranging from M -1.6 to 4.3 (Figure 3, top panel). The majority (75%) of events are micro-seismic events with magnitudes of 1 or smaller; only 74 events have magnitudes larger or equal to 2.5 of which only 4 are larger or equal to 3.5.

2. METHOD

The Gutenberg-Richter relationship given as

$$\log N = a - b \cdot M$$

where N is the number of events above a threshold magnitude M and a and b are empirical parameters. The parameter a describes the productivity of a sequence and b the relationship between the magnitudes of the sequence. High b-values indicate an abundance of small magnitude events and lower values more large magnitude events. It is often believed that an overall b-value should be close to one. However, this is often only the case for natural seismicity sampled over a large enough volume. Studies of seismicity related to magma intrusion (Wiemer and McNutt, 1997)) and geothermal projects (Bachmann et al, 2011, 2012), indicate that larger b-values and spatial and temporal variations can be associated with fluid-induced activity.

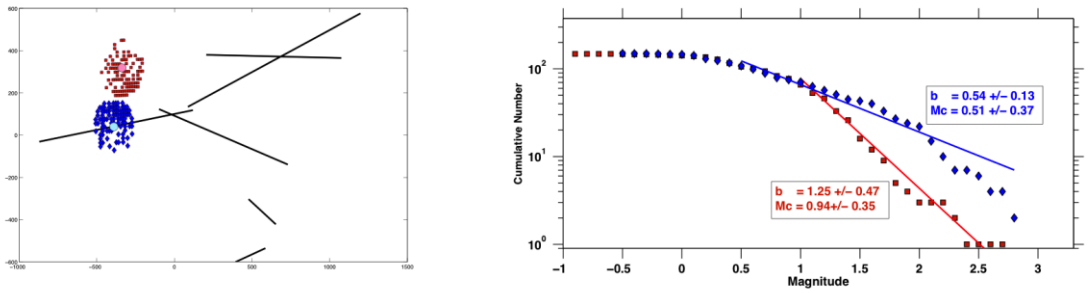

Figure 4: Illustration of mapping technique for 2D b-value mapping. The red and blue events represent the data that is sampled to determine the b-value at the light red and light blue location, respectively. The frequency-magnitude distributions of both sequences are shown in the second panel.

We determine temporal and spatial variations of the frequency-magnitude distribution (FMD). To determine spatial variations of the b-values, we apply a mapping technique introduced by Bachmann et al., 2012, which uses the nearest neighbors of events to determine local b-values. We adapt this technique for 2D mapping to determine relationships between faults and b-values. In figure 4, we illustrate the mapping technique. Around each event location we sample N events and require at least Y of those to have magnitudes above the local completeness threshold Mc to determine a local b-value. We here use N=150 and Y=25; a higher Y leads to similar patterns but to more locations where the local b-value cannot be determined. Blue and red in Figure 4 illustrates samples with low and high b-values, respectively.

To determine the temporal variations in the b-value, we divide the seismicity into the different injection phases defined above. We restrict our FMD analysis to the main seismic cloud shown in Figure 5. The coordinates in Figure 5 are relative to the injection well at (0/0) and the locations of the faults inferred by Ake et al. are shown as grey lines. The second panel of Figure 5 includes the events closest to the well (within the red box in the left panel), which we analyze first in our spatial analysis (see section 3.2).

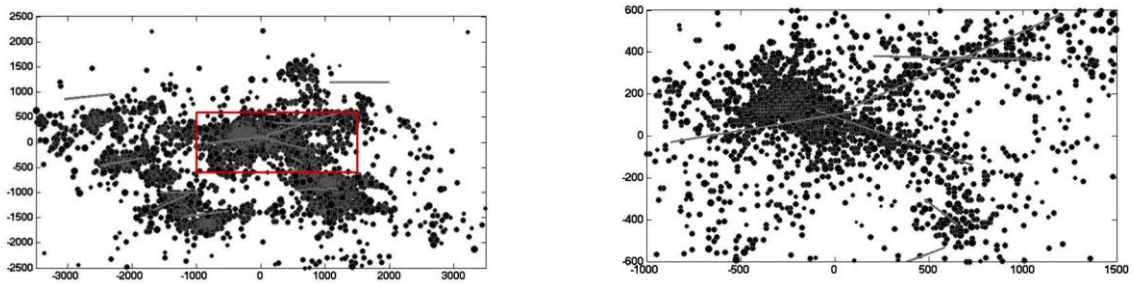

Figure 5: Seismic events of the Paradox Valley dataset, with two subsets; the location of the second subset is marked with a red square. Dark grey lines indicate faults as inferred by Ake et al., 2005.

3. RESULTS

3.1 Temporal variations of the statistical parameters

We summarize the temporal frequency-magnitude analysis in Table 1; all of those results are based on the main seismic cloud, shown in the first panel of Figure 5. There are two main findings: 1) The b-values decrease significantly after the initial injection tests; 2) while the b-values do not change significantly during the different later phases, the a-value decreases progressively from period to period. Analyzing the smaller subset (Figure 5, right panel) leads to similar, but less robust, results, as the number of events occurring during each period is smaller. We therefore do not include those results here.

Table 1: Temporal FMD analysis for the main seismic cloud (Figure 6, first panel).

Period	# Events	b-value	Mc	a-value (annual)
Injection Test	684	0.94+/-0.05	0.42+/-0.06	2.46
Continuous Injection	3884	0.66+/-0.02	0.33+/-0.06	2.44
Phase I	2555	0.73+/-0.02	0.33+/-0.06	3.01

Phase II	406	0.72+/-0.04	0.42+/-0.08	2.7
Phase III	180	0.74+/-0.09	0.51+/-0.16	2.4
Phase IV	703	0.66+/-0.14	0.82+/-0.36	2.13

While the b-values in this study are significantly smaller than the ones found from the geothermal study in Basel, Switzerland, we observe also in that case that the highest values occurred at the start of the injection. This is important for projects in general, as it cannot be assumed that high b-values, and thus small probabilities of large events, will be maintained as the injection proceeds. We propose that those patterns will be found in future projects as well. Due to the abundance of the small events during early injections, large b-values will be observed which should not be expected later on. Basel, it has been shown (Bachmann et al., 2011, 2012) that the b-values decreased after the injection terminated. This can't yet be tested for PV, as the injection is ongoing. Due to the other similarities with the induced seismicity in Basel, we propose that this would be found in PV as well.

The decrease in the a-value indicates that overall the injection strategies have been largely successful in mitigating induced seismicity at Paradox Valley, which offers some encouragement to operators in general. We also see that the completeness magnitude threshold (M_c in Table 1) for the network increased with time. This is counterintuitive as more stations were added with time and thus the monitoring should be better. On possible explanation is that with time the procedures changed and less attention was given to picking the smallest events...

Our results also indicate that the errors in the calculations increase with time, which is most apparent for Phase IV. While 703 events should be a large enough event number to determine a significant b-value and magnitude of completeness, the uncertainty is highest there. This indicates that we might be sampling over different processes with different dominant b-values. We can resolve this by the spatial mapping, which will be shown in the next section.

3.2 Spatial variations of the b-values

To determine spatial variations, we use the mapping technique explained in Figure 4 to determine local b-values. We start by introducing the results of the smaller subset (second panel in Figure 5), as the apparent fault structures are better defined closest to the injection well.

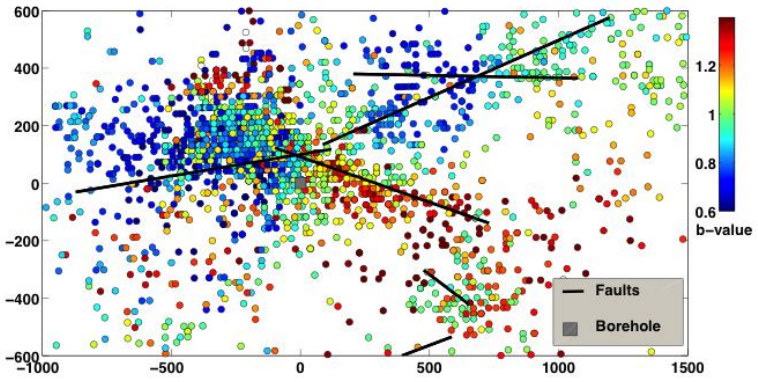

Figure 6: b-value analysis of the smaller subset. Faults inferred by Ake et al, 2005 are indicated in black.

We find that the pattern of b-values correlates with the inferred faults. We find that different faults have different dominant b-values around them. While it is difficult to determine the b-value of a fault directly as either there are too few events close to the faults or the faults are not defined well enough by the seismicity, we here can see a distinct pattern. While the faults aligned EW, favorably oriented for shear activation within the regional stress field,,, show smaller b-values (blue colors), the few fault with a more NW-SE orientation show higher b-values (red colors).

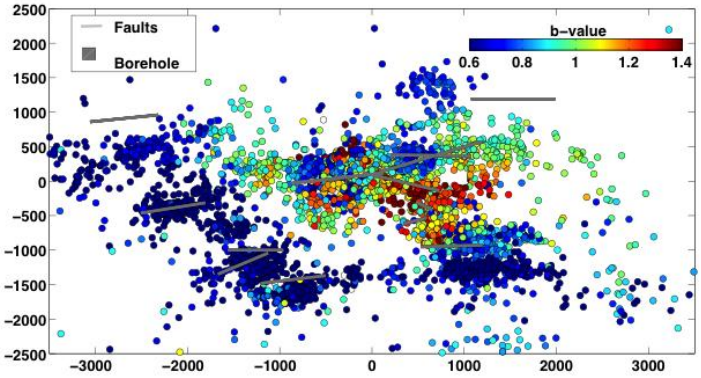

Figure 7: b-value analysis of the main seismic cloud. Faults inferred by Ake et al, 2005 are indicated in black

This pattern is seen even more clearly if we extend the map to the main seismic cloud and hence the data that was used for the temporal analysis. We see that all EW-aligned faults are dominated by smaller b-values.

Another pattern we see here is that high b-values only occur in close proximity to the borehole. This is again comparable to the results of the b-value analysis from Basel where the b-values decreased with distance to the injection point (Bachmann et al., 2012).

4. DISCUSSION AND CONCLUSIONS

We show here a statistical analysis of the Paradox Valley induced seismic sequence. This sequence has been active for over 20 years and includes close to 6,000 seismic events. The Paradox Valley injection serves as a proxy for proposed Geological Carbon Storage projects as they would have similar features, such as the long-term storage in the underground and the long-term injection of fluid.

Our study indicates that the patterns of the frequency-magnitude distributions of this sequence can be compared to that of the short-term geothermal project of Basel, Switzerland. This leads to the conclusion that this pattern might be expected at other projects as well. This is important for the risk assessment for future project as it helps to estimate the occurrence of large magnitude events. It is essential that the analysis from early seismic events will not simply be extrapolated as this would lead to a false security as early events show a significantly higher b-value.

By comparing the b-value pattern to the faults inferred by Ake et al., we find that there seems to be a correlation between the orientation of the faults and the size of the b-value. We find that while all faults oriented along the dominant EW direction show low b-values (blue colors in Figure 6 and 7), the only faults oriented in a less preferential NW-SW direction show higher b-values. One interpretation is that changes in pore pressure can only induce small magnitude events on this fault in a non-preferential direction. For future projects this would indicate that the largest magnitudes have to be expected in preferentially oriented faults. However, this result is only preliminary as there are too few faults to draw a solid conclusion. As mentioned above, the b-values tend to be high close to the injection well and the only fault in NW-SW direction is close by as well, which might cause this pattern. More studies on high-quality datasets are needed for clearer interpretations.

We restricted our analysis here on the main seismic cloud and did not discuss the seismicity to the North of the injection well. Such clusters can appear at any projects and it is can be difficult to model those beforehand. By analyzing the fault structures at a potential project side, the location of this cluster can maybe be predicted. However, the faults needed for such microseismicity are generally small, and thus they might not be detectable beforehand.

ACKNOWLEDGMENTS

We thank the US Bureau of Reclamation, especially L. Block, for access to the Paradox Valley data set. This study is part of the National Risk Assessment Partnership (NRAP).

REFERENCES

Ake, J., Mahrer, K., O'Connell, D., & Block, L. (2005). Deep-injection and closely monitored induced seismicity at Paradox Valley, Colorado. *Bulletin of the Seismological Society of America*, *95*(2), 664-683.

Bachmann, C. E., Wiemer, S., Woessner, J., & Hainzl, S. (2011). Statistical analysis of the induced Basel 2006 earthquake sequence: Introducing a probability- based monitoring approach for enhanced geothermal systems.*Geophysical Journal International*, *186*(2), 793-807.

Bachmann, C. E., Wiemer, S., Goertz- Allmann, B. P., & Woessner, J. (2012). Influence of pore- pressure on the event- size distribution of induced earthquakes. *Geophysical Research Letters*, *39*(9).

Ellsworth, W. L. (2013). Injection-induced earthquakes. *Science*, *341*(6142).

Giardini, D. (2009). Geothermal quake risks must be faced. *Nature*, *462*(7275), 848-849.

Gupta, H., (2002). A review of recent studies of triggered earthquakes by artificial water reservoirs with special emphasis on earthquakes in Koyna, India, *Earth Science Reviews* , 58 , 279–310.

Horton, S. (2012). Disposal of hydrofracking waste fluid by injection into subsurface aquifers triggers earthquake swarm in central Arkansas with potential for damaging earthquake. *Seismological Research Letters*, *83*(2), 250-260.

Keranen, K. M., Savage, H. M., Abers, G. A., & Cochran, E. S. (2013). Potentially induced earthquakes in Oklahoma, USA: Links between wastewater injection and the 2011 Mw 5.7 earthquake sequence. *Geology*, *41*(6), 699-702.

Simpson, D. W. (1986). Triggered earthquakes. *Annual Review of Earth and Planetary Sciences*, *14*, 21.

Talwani, P. (1998). On the nature of reservoir-induced seismicity. In *Seismicity Associated with Mines, Reservoirs and Fluid Injections* (pp. 473-492). Birkhäuser Basel.

Wiemer, S. & McNutt, S., (1997). Variations in the frequency-magnitude distribution with depth in two volcanic areas: Mount St Helens, Washington, and Mt Spurr, Alaska, *Geophys. Res. Let.* , 24 (2), 189–192.

Zoback, M. D., & Gorelick, S. M. (2012). Earthquake triggering and large-scale geologic storage of carbon dioxide. *Proceedings of the National Academy of Sciences*, *109*(26), 10164-10168.